

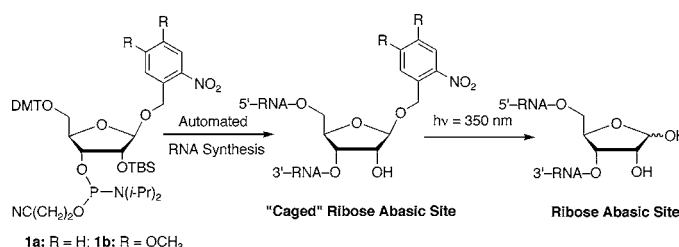
Photochemical Generation of Ribose  
Abasic Sites in RNA Oligonucleotides

John D. Trzupsek and Terry L. Sheppard\*

*Department of Chemistry and The Robert H. Lurie Comprehensive Cancer Center,  
Northwestern University, 2145 Sheridan Road, Evanston, Illinois 60208-3113**t-sheppard@northwestern.edu*

Received January 19, 2005

## ABSTRACT



A general method for the photochemical generation of ribose abasic sites within RNA oligonucleotides is reported. Photochemically caged nucleoside phosphoramidite analogues were prepared and incorporated into RNA oligonucleotides by automated RNA synthesis. Irradiation of the modified RNA at 350 nm efficiently produced ribose abasic sites at specific sites within RNA sequences. The current approach offers a chemical route to RNA abasic lesions for RNA biochemical studies.

The discovery of the *Tetrahymena* self-splicing intron<sup>1</sup> and the catalytic RNA of RNase P<sup>2</sup> highlighted RNA's dual role as an informational and catalytic macromolecule. Since then, RNA structural biology has shown that RNA adopts complex folded structures, reminiscent of proteins. In particular, the solution of the three-dimensional structure of the ribosome<sup>3</sup> has demonstrated that RNA molecules play a catalytic role in the chemistry of peptide bond formation in all cells.<sup>4</sup>

Pairing and stacking of nucleotide bases plays an important role in defining the three-dimensional structure, and resulting function, of DNA and RNA.<sup>5</sup> Thus, the preservation of

nucleotide chemical structure is essential for maintaining the integrity of the genome and gene expression. For this reason, DNA damage and repair mechanisms have received considerable recent attention.<sup>6</sup> For example, DNA "abasic sites", which result from hydrolysis of nucleotide *N*-glycosidic bonds or oxidation of sugar moieties in DNA nucleotides,<sup>7</sup> are premutagenic lesions that stall DNA and RNA polymerases.<sup>8</sup> DNA repair enzymes have evolved to excise abasic lesions and facilitate insertion of the correct nucleotide at the damage site.

RNA damage and repair mechanisms, in contrast, have received considerably less attention. Ribose abasic sites (**Z**, Scheme 1), resulting from *N*-glycosidic bond cleavage in RNA, may interfere with RNA coding and folding. RNA abasic sites are generated in cellular RNA by a class of

(1) Kruger, K.; Grabowski, P. J.; Zaug, A. J.; Sands, J.; Gottschling, D. E.; Cech, T. R. *Cell* **1982**, *31*, 147–157.

(2) Guerrier-Takada, C.; Gardiner, K.; Marsh, T.; Pace, N.; Altman, S. *Cell* **1983**, *35*, 849–857.

(3) (a) Ban, N.; Nissen, P.; Hansen, J.; Moore, P. B.; Steitz, T. A. *Science* **2000**, *289*, 902–921. (b) Yusupov, M. M.; Yusupova, G. Z.; Baucom, A.; Lieberman, K.; Earnest, T. N.; Cate, J. H. D.; Noller, H. F. *Science* **2001**, *292*, 883–896. (c) Harms, J.; Schlutzen, F.; Zarivach, R.; Bashan, A.; Gat, S.; Agmon, I.; Bartels, H.; Franceschi, F.; Yonath, A. *Cell* **2001**, *107*, 679–688.

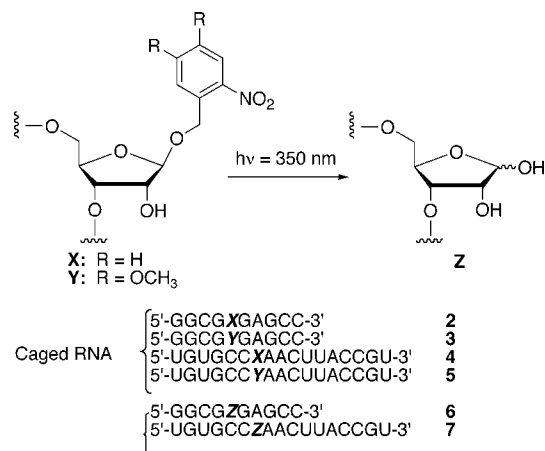
(4) (a) Nissen, P.; Hansen, J.; Ban, N.; Moore, P. B.; Steitz, T. A. *Science* **2000**, *289*, 920–930. (b) Moore, P. B.; Steitz, T. A. *Annu. Rev. Biochem.* **2003**, *72*, 813–850.

(5) Saenger, W. *Principles of Nucleic Acid Structure*; Springer-Verlag: New York, 1984.

(6) (a) Lukas, J.; Bartek, J. *Cell* **2004**, *118*, 666–668. (b) Sancar, A.; Lindsey-Boltz, L. A.; Uensal-Kacmaz, K.; Linn, S. *Annu. Rev. Biochem.* **2004**, *73*, 39–85.

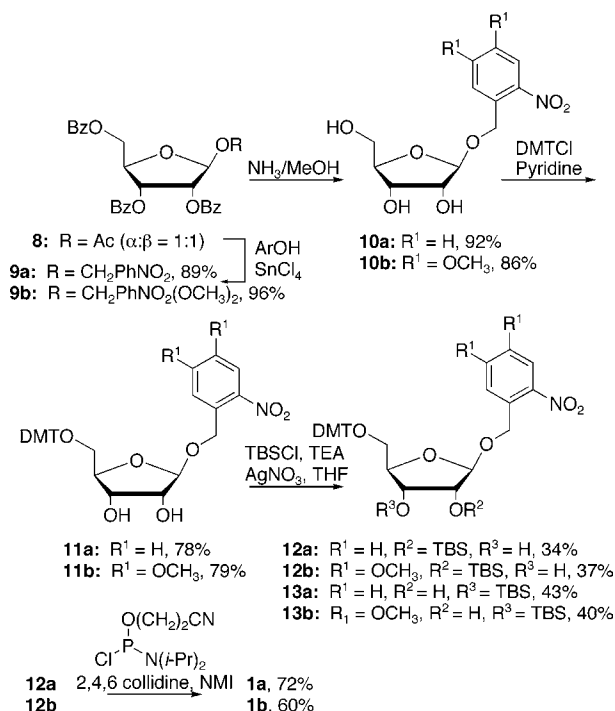
(7) Lhomme, J.; Constant, J. F.; Demeunynck, M. *Biopolymers* **2000**, *52*, 65–83.

(8) (a) Kroeger, K. M.; Jiang, Y. L.; Kow, Y. W.; Goodman, M. F.; Greenberg, M. M. *Biochemistry* **2004**, *43*, 6723–6733. (b) Berthet, N.; Roupioz, Y.; Constant, J. F.; Kotera, M.; Lhomme, J. *Nucleic Acids Res.* **2001**, *29*, 2725–2732. (c) Shibutani, S.; Takeshita, M.; Grollman, A. P. *J. Biol. Chem.* **1997**, *272*, 13916–13922.

**Scheme 1.** Photochemical Generation of Ribose Abasic Sites

*N*-glycosylase proteins called ribosomal inactivating proteins (RIPs).<sup>9</sup> A prototypic example is the toxin ricin.<sup>10</sup> The ricin A-chain (RA) targets ribosome inactivation by specific depurination of A<sub>4324</sub> in the 28S ribosomal RNA (rRNA). Structural studies of the sarcin/ricin (S/R) loop<sup>11</sup> demonstrated that A<sub>4324</sub> plays a critical role in molecular recognition within the ribosome. Thus, the generation of a ribose abasic site by ricin blocks ribosomal translocation and leads to cell death.<sup>12</sup> The importance of A<sub>4324</sub> was further underscored by a recent report of an RNA repair mechanism for the S/R rRNA domain.<sup>13</sup>

To facilitate biochemical studies of the ribosome and RIP action, we developed a chemical method for the generation of ribose abasic sites within RNA. A nonnatural tetrahydrofuran mimic of ribose abasic sites has been prepared.<sup>14</sup> Although this analogue serves as an effective model system,<sup>15</sup> it does not contain the C-1' hemiacetal functionality observed in natural ribose abasic sites. A current approach to ribose abasic sites involves treatment of target RNAs with an RIP, which is limited by the specificity and availability of the enzyme.<sup>16</sup> On the basis of methods for the site-specific generation of DNA aldehyde<sup>17</sup> and oxidized abasic sites,<sup>18</sup> we now report a photochemical method for the introduction

**Scheme 2.** Synthesis of Phosphoramidites **1a** and **1b**

of unique ribose abasic sites within RNA oligonucleotides. We describe the synthesis of two C-1 “caged” analogues (**1a** and **1b**, Scheme 2), their incorporation into RNA oligonucleotides by solid-phase RNA synthesis, and efficient photolytic deprotection to produce ribose abasic sites (Scheme 1).

Two target phosphoramidites (**1a** and **1b**, Scheme 2) were selected as precursors of ribose abasic sites. Each analogue contained a C-1 benzyl ether to enable selective photochemical release of the desired abasic site. The synthesis of the nitrobenzyl phosphoramidite (**1a**, Scheme 2) commenced with SnCl<sub>4</sub>-promoted glycosidation of **8** to yield the anomerically pure, protected ribofuranoside **9a** in 89% yield. The ribofuranoside **10a** was prepared by ammonolysis of the benzoyl protecting groups. Regioselective tritylation of **10a** was accomplished by slow addition of DMTCl, affording the desired ether **11a** in good yield. Silylation conditions, based on reported methods,<sup>19</sup> yielded a mixture of the 2'-*O*-silyl nucleoside (**12a**) and the isomeric 3'-*O*-silyl analogue (**13a**). The desired 2'-*O*-isomer (**12a**) was isolated by chromatography and converted to **1a** by standard RNA phosphitylation conditions.<sup>20</sup> The 3'-*O*-silyl isomer (**13a**) was utilized for the preparation of a solid-supported analogue for the synthesis of 3'-terminal caged RNA.<sup>21</sup> Analogue **1b**, which was based on the nitroveratryl protection group, was prepared by a parallel synthetic route (Scheme 2).

(18) (a) Kotera, M.; Bourdat, A.-G.; Defrancq, E.; Lhomme, J. J. *Am. Chem. Soc.* **1998**, *120*, 11810–11811. (b) Tronche, C.; Goodman, B. K.; Greenberg, M. M. *Chem. Biol.* **1998**, *5*, 263–271. (c) Lenox, H. J.; McCoy, C. P.; Sheppard, T. L. *Org. Lett.* **2001**, *3*, 2415–2418.

(19) Allerson, C. R.; Chen, S. L.; Verdine, G. L. *J. Am. Chem. Soc.* **1997**, *119*, 7423–7433.

(20) Scaringe, S. A.; Francklyn, C.; Usman, N. *Nucleic Acids Res.* **1990**, *18*, 5433–5441.

(9) (a) Girbes, T.; Ferreras, J. M.; Arias, F. J.; Stirpe, F. *Mini-Rev. Med. Chem.* **2004**, *4*, 461–476. (b) Barbieri, L.; Battelli, M. G.; Stirpe, F. *Biochim. Biophys. Acta* **1993**, *1154*, 237–282.

(10) Hartley, M. R.; Lord, J. M. *Biochim. Biophys. Acta* **2004**, *1701*, 1–14.

(11) (a) Szewczak, A. A.; Moore, P. B. *J. Mol. Biol.* **1995**, *247*, 81–98. (b) Correll, C. C.; Munishkin, A.; Chan, Y.-L.; Ren, Z.; Wool, I. G.; Steitz, T. A. *Proc. Natl. Acad. Sci. U.S.A.* **1998**, *95*, 13436–13441.

(12) (a) Montanaro, L.; Sperti, S.; Stirpe, F. *Biochem. J.* **1973**, *136*, 677–684. (b) Montanaro, L.; Sperti, S.; Mattioli, A.; Testoni, G.; Stirpe, F. *Biochem. J.* **1975**, *146*, 127–131.

(13) Ogasawara, T.; Sawasaki, T.; Morishita, R.; Ozawa, A.; Madin, K.; Endo, Y. *EMBO J.* **1999**, *18*, 6522–6531.

(14) Beigelman, L.; Karpeisky, A.; Usman, N. *Bioorg. Med. Chem. Lett.* **1994**, *4*, 1715–1720.

(15) Peracchi, A.; Beigelman, L.; Usman, N.; Herschlag, D. *Proc. Natl. Acad. Sci. U.S.A.* **1996**, *93*, 11522–11527.

(16) Amukele, T. K.; Schramm, V. L. *Biochemistry* **2004**, *43*, 4913–4922.

(17) (a) Groebke, K.; Leumann, C. *Helv. Chim. Acta* **1990**, *73*, 608–617. (b) Peoc'h, D.; Meyer, A.; Imbach, J. L.; Rayner, B. *Tetrahedron Lett.* **1991**, *32*, 207–210. (c) Shishkina, I. G.; Johnson, F. *Chem. Res. Toxicol.* **2000**, *13*, 907–912.

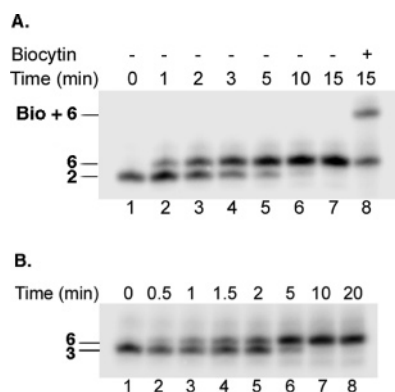


**Figure 1.** Photochemical generation of ribose abasic sites. 5'-Radiolabeled oligonucleotide (**2** or **3**) was irradiated at 350 nm in phosphate-buffered saline (PBS) buffer and analyzed by 20% dPAGE. (A) Nitrobenzyl-caged RNA (**2**) remaining was 93%, 70%, 49%, 36%, 23%, 10%, and 7% for lanes 1–7, respectively. Lane 8: reaction with biocytin hydrazide (5 mM final concn, 95 °C, 30 min, 57% conversion). (B) Nitroveratryl-caged RNA (**3**) remaining was 89%, 75%, 61%, 56%, 53%, 25%, 14%, and 10% for lanes 1–8, respectively.

Several model RNA sequences were designed to demonstrate the use of analogues **1a** and **1b** for the synthesis of ribose abasic sites. Sequences **2** and **4** contained the nitrobenzyl-caged abasic site at position X (from **1a**, Scheme 1). Oligonucleotide **2** was designed as a mimic of the S/R domain in 28S rRNA, and oligonucleotide **4** served as a longer sequence to validate the method. Sequences **3** and **5** were analogous to **2** and **4**, respectively, but were prepared with the nitroveratryl analogue, **1b** (**Y**, Scheme 1).

Phosphoramidite analogues **1a** and **1b** were used to introduce the caged analogues into RNA oligonucleotides (**2** and **4** or **3** and **5**, respectively) by standard RNA solid-phase synthesis methods.<sup>22</sup> Analogue **1a** was incorporated in modest yield (53%), even with enhanced coupling times. However, **1b** was introduced with high coupling yields (98%). RNA nucleotide coupling yields were ~98% after introduction of each caged analogue.

Caged oligonucleotides **2–5** were deprotected using standard conditions: RNA was treated with 28% NH<sub>4</sub>OH/EtOH for 24 h followed by immediate desilylation. Standard TBAF desilylation conditions<sup>20</sup> led to modified RNA products. However, deprotection with triethylamine trihydrofluoride (TEA·3HF, ~24 h at 65 °C) provided RNA products cleanly. Deprotected oligonucleotides were purified by denaturing polyacrylamide gel electrophoresis (20% dPAGE; 29:1 acrylamide/bisacrylamide, 8 M urea), followed by reverse-phase HPLC (RP-HPLC). A single oligonucleotide product was observed after purification. RNA oligonucleotides **2–5** were characterized by mass spectrometry (MALDI-TOF MS). All caged oligonucleotides showed the expected molecular masses (see Supporting Information).

dPAGE analysis was used to evaluate the efficiency of photolytic deprotection of oligonucleotides **2** and **3** to produce RNA containing a unique ribose abasic site (**6**, **Z**

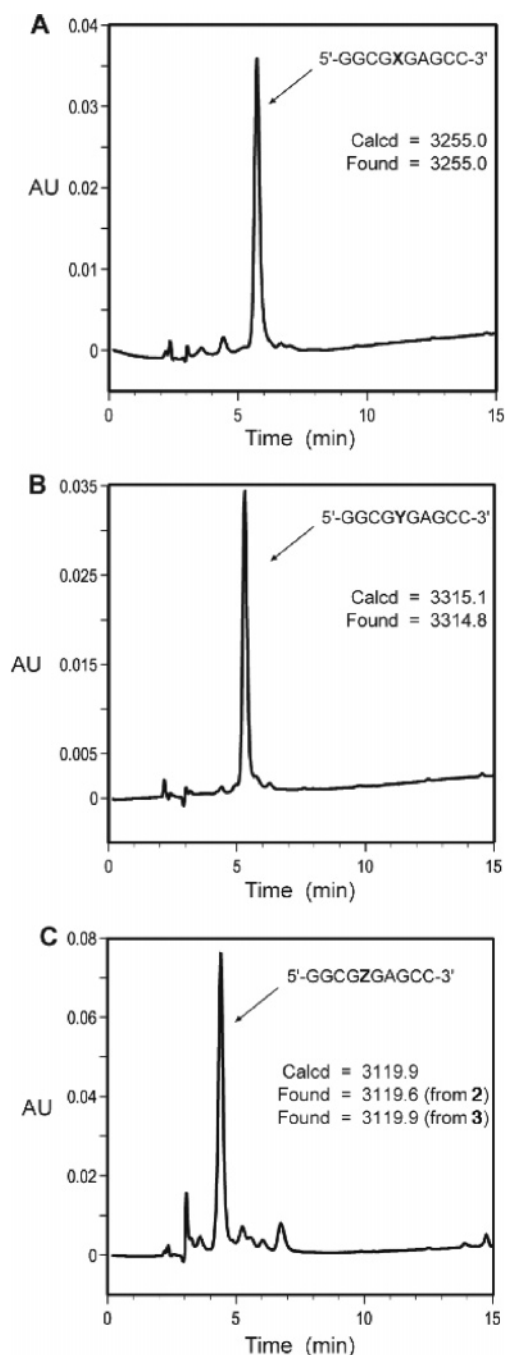


**Figure 2.** RP-HPLC and MALDI-TOF MS characterization of photochemical deprotection for (A) oligonucleotide **2** and (B) oligonucleotide **3**. (C) Products from photolytic cleavage of each caged species (**2** and **3**) were combined and coinjected. Retention times of the corresponding oligonucleotides were 5.7, 5.3, and 4.4 min for **2**, **3**, and **6**, respectively.

in Scheme 1). Oligonucleotides **2** and **3** were 5'-radiolabeled and independently irradiated at 350 nm. Reaction aliquots were removed at specific times and analyzed by dPAGE. As shown in Figure 1, caged RNAs **2** (Figure 1A) and **3** (Figure 1B) underwent a time-dependent gel mobility shift upon UV irradiation. Deprotection half-lives of 2.3 min (**2**) and 2.2 min (**3**) were determined by quantification of the

gel image. To support a preliminary assignment of **6**, oligonucleotides **2** and **3** were irradiated and treated with the aldehyde-reactive probe, biocytin hydrazide (BH). BH was designed to trap aldehyde abasic sites by hydrazone formation.<sup>23</sup> Caged **2** or **3** remained unmodified by BH (<1% hydrazone formation). However, decaging of oligonucleotide **2** or **3** led to a product that was efficiently labeled by BH (lane 8, Figure 1A). Caged oligonucleotides **4** and **5** also were subjected to photolytic treatment and gel electrophoretic analysis. Due to the greater length of **4** and **5**, the corresponding product oligonucleotide (**7**, Scheme 1) comigrated with the starting oligonucleotides during gel analysis. However, **4** and **5** displayed a UV-induced, time-dependent gel mobility shift when incubated with BH (Supporting Information). The gel electrophoresis and chemoselective labeling system provided validation of the approach (Scheme 1), but more rigorous characterization standards were applied.

Formation of ribose abasic sites in RNA oligonucleotides was validated directly by RP-HPLC and MALDI-TOF MS analysis. Caged oligonucleotides **2** and **3** exhibited RP-HPLC retention times of 5.7 and 5.3 min, respectively (Figures 2A and 2B). After UV irradiation (350 nm) for 25 min, each oligonucleotide was quantitatively converted to a single peak with a retention time of 4.4 min. Products from the decaging reactions of **2** and **3** were isolated, mixed, and subjected to RP-HPLC analysis. The products coeluted with a retention time of 4.4 min (Figure 2C), indicating that they were identical. In a separate experiment, oligonucleotides **2** and **3** were irradiated, and the resulting products were purified and characterized by mass spectrometry. MALDI-TOF MS analysis of the decaged products resulted in  $m/z$  values of 3119.6 for **2** and 3119.9 for **3**, which were in excellent agreement with the predicted mass for **6** ( $m/z = 3119.9$ ). Oligonucleotides **4** and **5** were subjected to a parallel RP-HPLC and MALDI-TOF MS analysis (Supporting Information). RP-HPLC coinjection experiments demonstrated that, upon irradiation, **4** and **5** produced the same product, which had the mass expected for **7** (calcd 5229.1  $m/z$ ; found 5229.1 (**4**) and 5229.8 (**5**)).

Further analysis showed that ribose abasic sites in RNA, like their DNA counterparts,<sup>15</sup> readily underwent strand scission by  $\beta$ -elimination. For example, when purified **6** was concentrated to dryness, three peaks with retention times of 3.0, 3.3, and 4.4 min were observed by RP-HPLC. MALDI-TOF MS data for the two major products were in good agreement with the masses expected for  $\beta$ -elimination at position **Z**. Thus, to avoid strand scission, oligonucleotides containing ribose abasic sites should be handled at low temperatures and under controlled conditions.

In summary, we have developed a general method for the site-specific introduction of ribose abasic sites within RNA oligonucleotides. Using a caged phosphoramidite reagent, a stable nucleotide analogue was introduced into RNA by solid-phase synthesis. The ribose abasic site lesion was subsequently revealed by UV irradiation. The system permits the insertion of ribose abasic sites at any site within an RNA oligonucleotide, which will provide a new reagent for RIP mechanistic studies. With appropriate modification, our approach should be compatible with other high-yielding RNA synthesis strategies.<sup>24</sup> In addition, our method, combined with standard RNA splint–ligation methods,<sup>25</sup> should permit studies of ribose abasic sites within large RNAs. Finally, the C-1 aldehyde of the ribose abasic site may offer a unique chemical handle for chemoselective modification reactions within RNA sequences.<sup>26</sup>

**Acknowledgment.** This work was supported by the Robert H. Lurie Comprehensive Cancer Center of Northwestern University. The MALDI-TOF mass spectrometer was purchased with funds provided by an NIH Scientific Instrumentation grant (1-S10-RR13810).

**Supporting Information Available:** Detailed experimental protocols and spectral data for all compounds. This material is available free of charge via the Internet at <http://pubs.acs.org>.

OL050120H

(21) *Oligonucleotide Synthesis A Practical Approach*, Gait, M. J., Ed.; Oxford University Press: Washington, DC, 1985.

(22) Wincott, F.; DiRenzo, A.; Shaffer, C.; Grimm, S.; Tracz, D.; Workman, C.; Sweedler, D.; Gonzalez, C.; Scaringe, S.; Usman, N. *Nucleic Acids Res.* **1995**, *23*, 2677–2684.

(23) Ide, H.; Akamatsu, K.; Kimura, Y.; Michiue, K.; Makino, K.; Asaeda, A.; Takamori, Y.; Kubo, K. *Biochemistry* **1993**, *32*, 8276–8283.

(24) Scaringe, S. A.; Wincott, F. A.; Caruthers, M. H. *J. Am. Chem. Soc.* **1998**, *120*, 11820–11821.

(25) Moore, M. J.; Sharp, P. A. *Science* **1992**, *256*, 992–997.

(26) For example, see: (a) Trévisiol, E.; Defrancq, E.; Lhomme, J.; Laayoun, A.; Cros, P. *Tetrahedron* **2000**, *56*, 6501–6510. (b) Dey, S.; Sheppard, T. L. *Org. Lett.* **2001**, *3*, 3983–3986.